International Symposium
On Turbulence and Shear Flow
Phenomena (TSFP-9)
June 30 - July 3, 2015 *Melbourne, Australia*

DIRECT NUMERICAL SIMULATION OF A TURBULENT PIPE FLOW WITH TEMPORAL ACCELERATION

Yongmann M. Chung
School of Engineering and Centre for Scientific Computing,
University of Warwick
Coventry, CV4 7AL, U.K.
Y.M.Chung@warwick.ac.uk

Zhixin Wang and Tariq Talha
School of Engineering and Centre for Scientific Computing,
University of Warwick
Coventry, CV4 7AL, U.K.

ABSTRACT

Turbulent pipe flows subject to temporal acceleration is considered in this study. Direct numerical simulations of accelerating turbulent pipe flow were performed to study the response of the turbulent structures to temporal acceleration. The simulations were started with the fully-developed turbulent pipe flow at an initial Reynolds number, and then a constant temporal acceleration was applied. During the acceleration, the Reynolds number based on the bulk-mean velocity and the diameter of the pipe increased linearly in time from the initial Reynolds number. The range of Reynolds numbers considered were $5300 \leq Re_D \leq 11\,700$. Instantaneous flow fields were analysed. It is found that the temporal acceleration initially weakened the flow structures before new turbulence was generated later in the near-wall region.

1 Introduction

Unsteady turbulent wall-bounded flows are frequently encountered in engineering applications such as turbomachinery and heat exchangers, and also in biomedical applications such as airflow in the human lungs and blood flows in large arteries. In addition to the practical implications of achieving a better understanding of flows of this type, the study of unsteady turbulent flows provides insight into the underlying physics of turbulent boundary layers. Most studies have considered the periodic turbulent flow, where the pressure gradient (or the mass flow rate) changes periodically in time. However, unsteady turbulent flows with temporal acceleration have received relatively little attention despite their importance (He & Jackson, 2000; Greenblatt & Moss, 2004; Chung, 2005, 2012).

Temporal acceleration/deceleration, where the change is imposed in time rather than in space, is different from the accelerating/decelerating boundary later. Turbulent boundary layer flows subjected to favourable pressure gradient (FPG) and adverse pressure gradient (APG) undergo spatial acceleration/deceleration. Previous studies have attempted to make comparisons between the boundary layer flows subjected to FPG/APG with the temporal transient flows and several similarities between temporal and spatial non-equilibrium flows have been found (Greenblatt & Moss, 1999, 2004).

Early studies of accelerating turbulent flow were mainly conducted experimentally, but detailed information on the changes in flow structures during temporal acceleration is not available due to technical difficulties (Greenblatt & Moss, 1999, 2004; He & Jackson, 2000). Numerical studies on the transient turbulent flow with temporal acceleration/deceleration are particularly scarce. Chung (2005) performed direct numerical simulations of a decelerating turbulent channel flow. A step decrease in pressure gradient was applied to impose a sudden deceleration. It was found that there were two different relaxations in the decelerated flow: a fast relaxation at the early stage and a slow one at the later stage. The anisotropic response of the near-wall turbulence was detected in the early stage, which would be a troublesome problem to standard turbulence models. Jung & Chung (2012) performed large-eddy simulations (LES) of accelerating turbulent flow. The simulation conditions were chosen to compare the experiments of He & Jackson (2000). The simulation started with an equilibrium turbulent flow at $Re_{D0} = 7000$ (or $Re_\tau = 230$). Turbulent pipe flow was then subjected to a constant temporal acceleration. The simulation terminated at the final Reynolds of $Re_{D1} = 35000$ (or $Re_\tau = 800$). The LES results identified the three delays observed in the experiment. Seddighi *et al.* (2014) reported a constant acceleration case between $Re_\tau = 180$ and 420.

Most of previous numerical studies have considered the channel flow, and the accelerating pipe flow was not investigated with an exception of LES study of Chung (2012); Jung & Chung (2012). In this study, unsteady turbulent pipe flows subject to temporal acceleration are presented, and the responses of various turbulent quantities are examined. Direct numerical simulations were performed for a Reynolds number range of $5300 \leq Re_D \leq 11\,700$. The aim of the present study is to investigate the response of the near-wall turbulence after temporal acceleration. Detailed turbulence statistics and conditional averaging have been generated which provides a clear understanding of the turbulence dynamics.

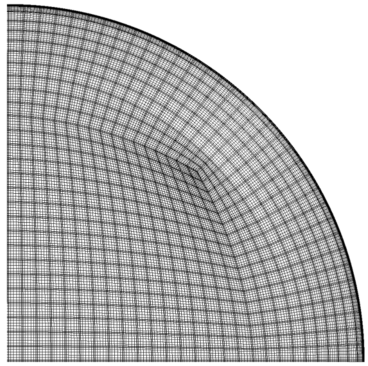

Figure 1. A quarter-section view of the spectral element mesh in $r-\theta$ plane used for $Re_\tau = 500$ simulation.

2 Numerical methods

For the pipe flow DNS, the incompressible Navier-Stokes equations were solved using a high-order spectral element method code nek5000 (Fischer *et al.*, 2008). The computational domain was divided into small local quadrilateral elements with Gauss-Lobatto-Legendre (GLL) points on each element. The velocity space was represented by a basis of Nth-order Lagrange polynomials on the GLL nodes, while for the pressure space the $N-2$ order of Lagrangian interpolants were used on the Gauss-Legendre quadrature points. This is known as the $P_N - P_{N-2}$ formulation proposed by Maday & Patera (1989). The time-marching scheme used in nek5000 was a semi-implicit method with the nonlinear terms treated explicitly using third order extrapolation (EXT3) while the viscous terms were treated implicitly by a third order backward differentiation (BDF3).

A periodic boundary condition was applied in the streamwise direction with a no-slip boundary condition applied on the pipe wall. The polynomial order for the velocity space was set to be 7 for all the simulation cases considered. In the steady turbulent pipe simulations, the mean pressure gradient was adjusted dynamically at each time step to maintain a constant bulk-mean velocity in the pipe. In the transient pipe simulations, the mean pressure gradient was adapted to allow the bulk-mean velocity to increase linearly during the whole acceleration process.

Figure 1 shows a cross-sectional view of the spectral element mesh used for the $Re_\tau = 500$ case. The GLL points within the element are clearly visible as highlighted. A total number of 832728 elements (with 426 million grid points) were used for the steady simulation at this Reynolds number. The resolutions used in this study were similar to those used in El-Khoury *et al.* (2013): $\Delta y^+_{max} \le 5$ with four grid points below $\Delta y^+ = 1$ and fourteen grid points below $\Delta y^+ = 10$, and $\Delta z^+_{max} \le 10$ and $\Delta r\theta^+_{max} \le 5$, respectively. A doughnut shape of mesh was chosen for the region 0.8 r/R 1 to improve the quality of the grid near the pipe wall, so that no extra interpolation is needed for the data processing within this near-wall region. Turbulence statistics such as vorticity, pressure and velocity up to 4th order were averaged along the axial direction, and resulting two-dimensional statistics were saved during the simulations.

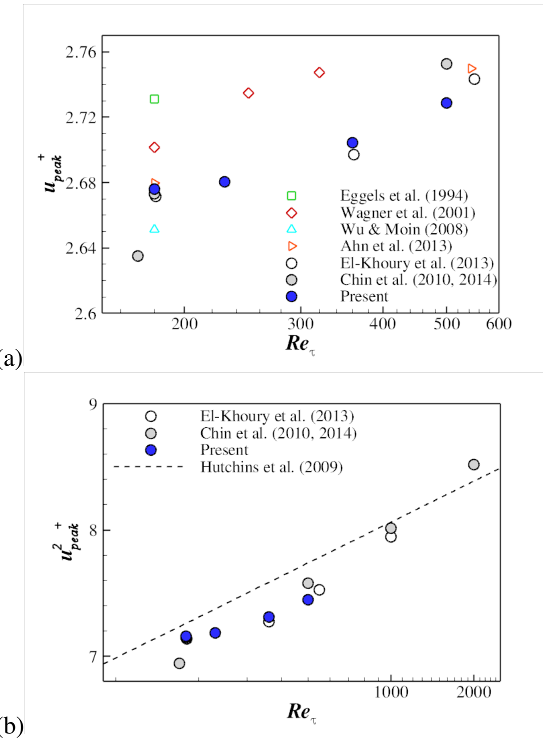

(a)

(b)

Figure 2. (a) Comparison of the maximum streamwise velocity fluctuation of turbulent pipe flows. Also included are data from Eggels *et al.* (1994); Wu & Moin (2008); Chin *et al.* (2010, 2014); Ahn *et al.* (2013); El-Khoury *et al.* (2013); Wagner *et al.* (2001). (b) Comparison of the peak axial turbulence intensity values from DNSs using spectral element method. Dashed line represents the correlation $u^{2+}_{peak} = 1.075\log_{10}(Re_\tau) + 4.837$ as proposed by Hutchins *et al.* (2009) for boundary layers.

3 Results and Discussion

3.1 Steady turbulent pipe flow

DNSs have been performed for steady turbulent pipe flows at four different Reynolds numbers. A pipe length of $30R$ was chosen for all four simulations in order to obtain converged turbulence statistics (Chin *et al.*, 2010), and also to accommodate the large scale structures. Velocity fluctuations are compared with previous DNS pipe flow data. Figure 2(a) shows the maximum of streamwise velocity fluctuation for each Reynolds number. Results from present turbulent pipe flow simulations agree very well with the DNS data in literature at comparable Reynolds numbers. It can also be observed that the maximum u_{rms} value increases with Reynolds number. This is in consistent with the other DNS studies on turbulent pipe and channel flows. In general, results of spectral element methods show good agreement with each other, while results from the other methods appear to over-predict the maximum u_{rms} value. In Figure 2(b), the maximum u_{rms} values are compared with other spectral element method DNS studies (Chin *et al.*, 2010, 2014; El-Khoury *et al.*, 2013). The formulation of the increasing u^2_{max} for turbulent boundary layers suggested by Hutchins *et al.* (2009) is also included for comparison. The present DNS data agree well with the results of El-Khoury *et al.* (2013), in which the nek5000 code was also used to resolve the turbulent flows. This demonstrates the adequacy

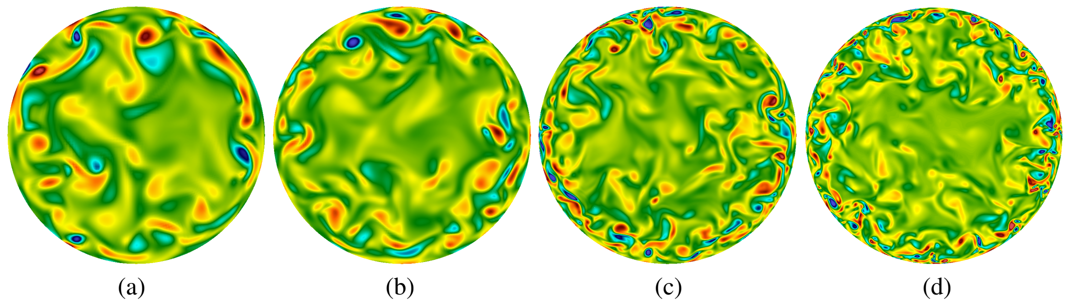

Figure 3. Contours of instantaneous streamwise vorticity (ω_x) in the circular pipe flow at various Reynolds numbers. (a) $Re_\tau = 180$, (b) $Re_\tau = 230$, (c) $Re_\tau = 360$ and (d) $Re_\tau = 500$. Red colour represents positive values and blue colour represents negative values.

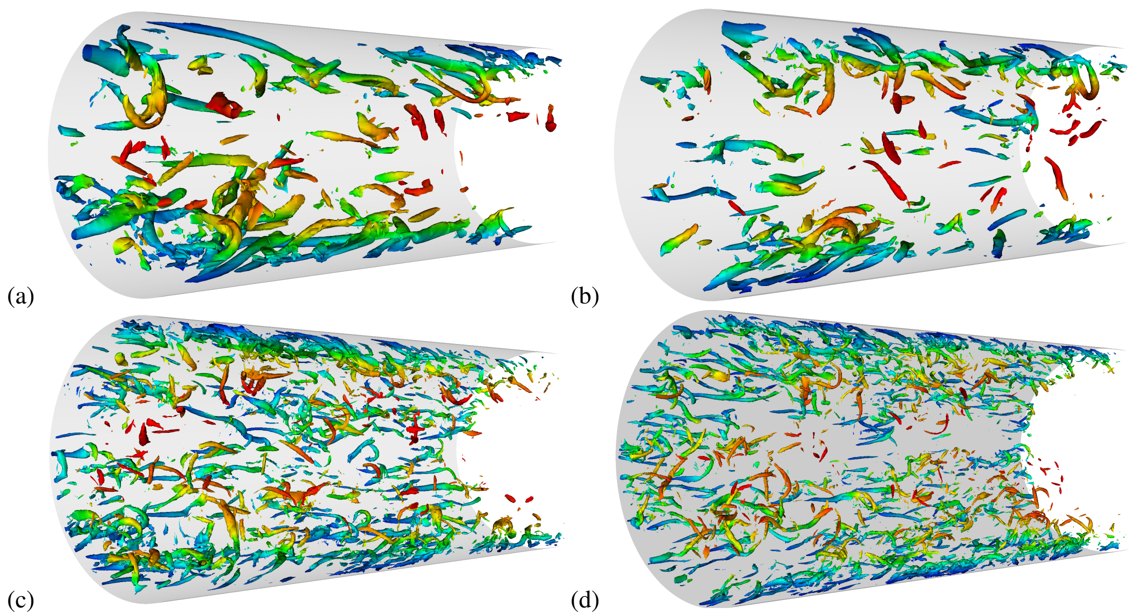

Figure 4. λ_2 structures in the circular pipe flow. (a) $Re_\tau = 180$, (b) $Re_\tau = 230$, (c) $Re_\tau = 360$ and (d) $Re_\tau = 500$. The structures are coloured by the distance from the pipe wall.

of the numerical methods used in the pipe flow simulation.

Figure 3 shows contours of the instantaneous streamwise vorticity. Details of the turbulent structures are clearly captured, and the flow structures become smaller as the Reynolds number increases. In particular, the sizes of the streamwise vortices in the near-wall region reduce significantly at higher Reynolds numbers. The turbulent structures are visualised in Figure 4 using λ_2 structures (Jeong & Hussain, 1995). The near-wall region of the pipe flow was populated with streamwise vortices.

3.2 Accelerating turbulent pipe flow

Now, the unsteady turbulent pipe flow subject to temporal acceleration was considered. The simulations were started from a fully-developed turbulent pipe flow at $Re_D = 5300$ (or $Re_\tau \approx 180$ based on the friction velocity u_τ and the radius R) (Chung, 2012). The acceleration parameter $a = 0.05$ (corresponding to $dRe_D/dt = 265$) was kept constant throughout the simulations, so the mass flow rate increased linearly to the final Reynolds number of 11 700 (or $Re_\tau \approx 360$). From the preliminary simulations, it was found that the acceleration parameter of $a = 0.05$ was strong enough to exhibit unsteady characteristics for the Reynolds number range considered.

As shown in Figure 5(a) the bulk-mean velocity increases linearly in time during the acceleration, and the Reynolds number ratio between the start and end of the acceleration is about $C_{Re} = 2.2$. During the acceleration, the mean wall shear stress shows a distinctive three-stage development in Figure 5(b): (1) the initial transient stage with the wall shear stress overshooting the corresponding steady values, (2) the weak transient stage with the wall shear stress much lower than the steady values, and (3) the strong transient stage with the wall shear stress increasing rapidly towards the steady values. Due to the acceleration range considered in this study, a pseudo-steady stage is not shown here. A similar response of wall shear stress was also observed in LES (Jung & Chung, 2012) and experimental (He *et al.*, 2011) study of transient pipe flow.

Figure 6 shows streamwise velocity contours in the $r-\theta$ plane at several Reynolds numbers during the acceleration. The same contour levels are used for all Reynolds numbers. The accelerating flow is clearly visualised with

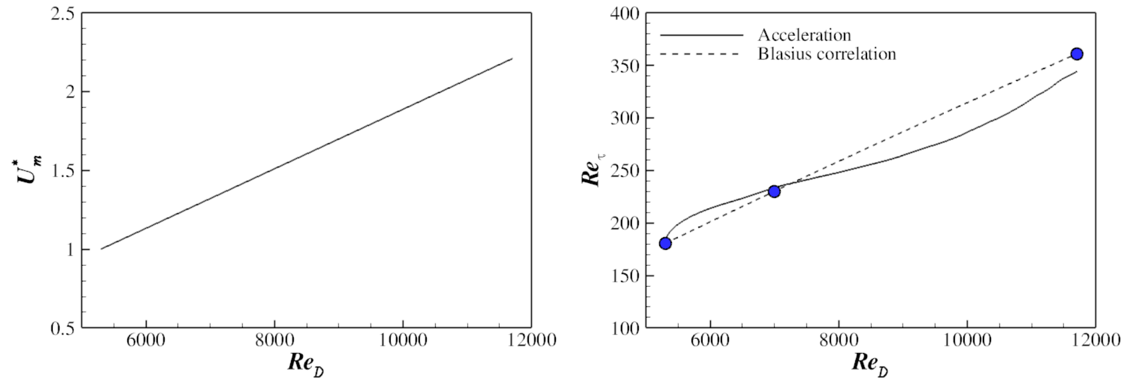

Figure 5. Time history of bulk mean velocity and wall shear stress during the linear acceleration. Symbols are the values from steady pipe flow simulations at $Re_D = 5300$, 7000 and 11700 respectively. Blasius' correlation is also included for comparison.

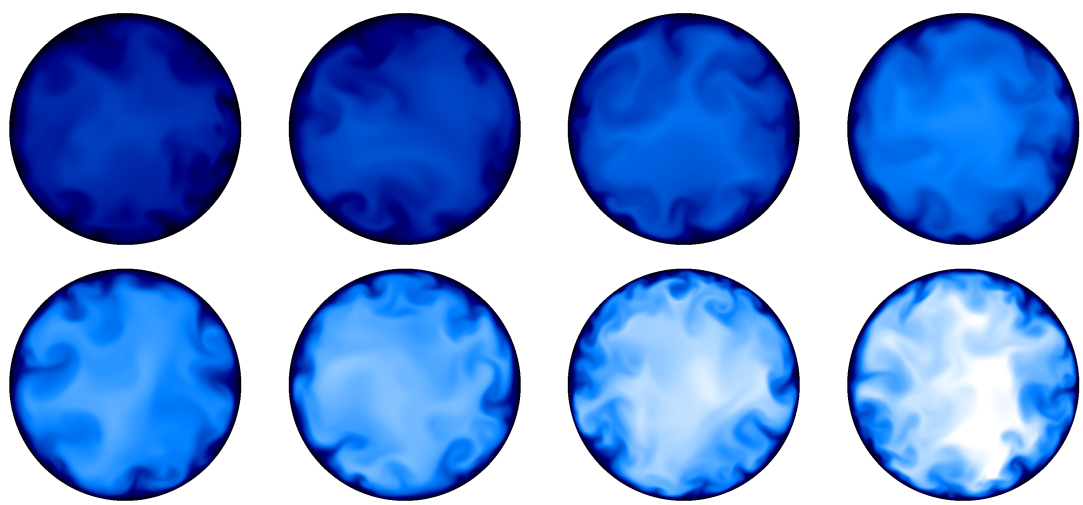

Figure 6. Instantaneous streamwise velocity contours during the acceleration. (a) $Re_D = 5300$; (b) $Re_D = 6000$; (c) $Re_D = 7000$; (d) $Re_D = 8000$; (e) $Re_D = 9000$; (f) $Re_D = 10000$; (g) $Re_D = 11000$; (h) $Re_D = 11700$. White colour represents high velocity and dark colour represents low velocity. The same contour levels are used for all the plots.

the thinning of the near wall layer. The low-speed streaks are shown in Figure 7. The initial streak spacing is about 100 in wall units, and the streaks become elongated with acceleration. At the later stage, stronger velocity fluctuations appear locally, suggesting the generation of new turbulence. This is in consistent with the behaviour of wall shear stress during the acceleration. In the later stage of the acceleration, the new structures gradually occupy the pipe wall region.

A similar trend can be observed in the evolution of the near-wall streamwise vortical structures. Figure 8 shows a combined view of the 2D instantaneous streamwise vorticity (ω_x) contours and the $\lambda_2 2$ structures during the acceleration. At the initial transient stage, the near-wall turbulent structures remain largely unchanged in terms of both size and strength, accompanied by the elongation of low-speed-streaks. As the acceleration continues, the structures become weakened and gradually disappear from certain areas of the near-wall region. In the later stage of the acceleration, new turbulent structures with smaller size and stronger strength emerge and gradually occupy the whole pipe wall region.

The new structures generated in the later stage of the acceleration are tracked as shown in the streamwise vorticity plots. It is worth noticing that the new turbulent structures appears at $Re_D = 8000$ near the bottom of the pipe ($\theta = 3\pi/2$), and gradually become smaller and stronger during the acceleration. New turbulence appears at the top of the pipe ($\theta = \pi/2$) at $Re_D = 9000$. From the instantaneous streamwise vorticity plots, it can be clearly seen that the overall turbulent structures become smaller and much stronger in the later stage. Note that due to the relatively short acceleration range considered in this study, the turbulent structures are yet to fully response at the end of the acceleration.

4 Conclusions

Direct numerical simulations of both steady and unsteady turbulent pipe flows are performed using the spectral element based solver, nek5000. Results from the steady flow simulations compared well with other DNS studies.

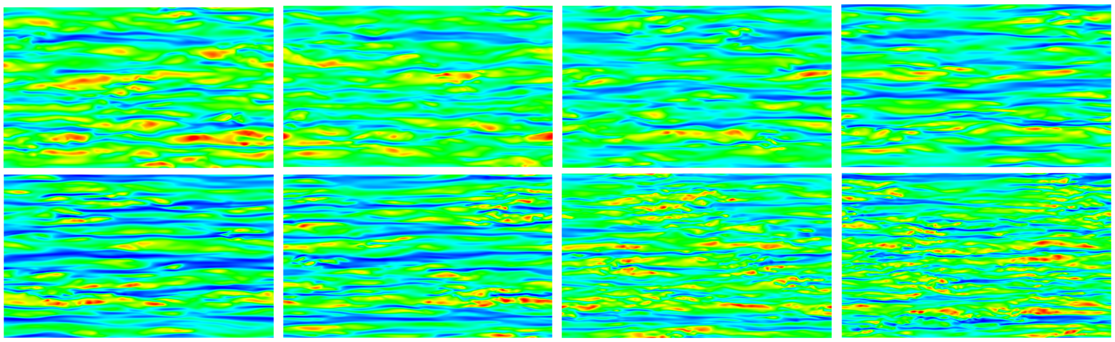

Figure 7. Low-speed-streaks in the pipe near-wall region during the acceleration: (a) $Re_D = 5300$; (b) $Re_D = 6000$; (c) $Re_D = 7000$; (d) $Re_D = 8000$; (e) $Re_D = 9000$; (f) $Re_D = 10000$; (g) $Re_D = 11000$; (h) $Re_D = 11700$. The cut planes are chosen at $y^+ \approx 10$ from the pipe wall based on the local u_τ and then unwrapped and presented in $x-\theta$ plane view.

Unsteady turbulent pipe flow subject to constant temporal acceleration is studied and a three-stage development of mean wall shear stress is observed. Further analyses on the evolution of turbulent structures and behaviour of low-speed-streaks have shown that stronger and smaller turbulent structures associated with higher Reynolds number coexist with the old structures. Further work will focus on the relationship between two different structures and also longer acceleration period and higher acceleration rates.

Acknowledgements

The financial support from the European Union Seventh Framework Programme FP7/2007-2013 AirPROM (Grant Agreement FP7 270194, www.airprom.eu) is acknowledged.

REFERENCES

Ahn, J., Lee, J. H., Jang, S. J. & Sung, H. J. 2013 Direct numerical simulations of fully developed turbulent pipe flows for Re_τ = 180, 544 and 934. *International Journal of Heat and Fluid Flow* **44**, 222–228.

Chin, C., Monty, J. P. & Ooi, A. 2014 Reynolds number effects in dns of pipe flow and comparison with channels and boundary layers. *International Journal of Heat and Fluid Flow* **45**, 33–40.

Chin, C., Ooi, A. S. H., Marusic, I. & Blackburn, H. M. 2010 The influence of pipe length on turbulence statistics computed from direct numerical simulation data. *Physics of Fluids* **22** (11), 115107.

Chung, Y. M. 2005 Unsteady turbulent flow with sudden pressure gradient changes. *International Jounal for Numerical Methods in Fluids* **47** (8-9), 925–930.

Chung, Y. M. 2012 Turbulent flow with temporal acceleration: A numerical study on turbulent structures. In *11th International Conference on Pressure Surges*. 24-26 October, Lisbon, Portugal.

Eggels, J. G. M., Unger, F., Weiss, M. H., Westerweel, J., Adrian, R. J., Friedrich, R. & Nieuwstadt, F. T. M. 1994 Fully-developed turbulent pipe-flow: A comparison between direct numerical simulation and experiment. *Journal of Fluid Mechanics* **268**, 175–209.

El-Khoury, G. K., Schlatter, P., Noorani, A., Fischer, P. F., Brethouwer, G. & Johansson, A. V. 2013 Direct numerical simulation of turbulent pipe flow at moderately high reynolds numbers. *Flow, Turbulence and Combustion* **91** (3), 475–495.

Fischer, P. F., Lottes, J. W. & Kerkemeier, S. G. 2008 nek5000 Web page, http://nek5000.mcs.anl.gov.

Greenblatt, D. & Moss, E. A. 1999 Pipe-flow relaminarization by temporal acceleration. *Physics of Fluids* **11** (11), 3478–3481.

Greenblatt, D. & Moss, E. A. 2004 Rapid temporal acceleration of a turbulent pipe flow. *Journal of Fluid Mechanics* **514**, 65–75.

He, S., Ariyaratne, C. & Vardy, A. E. 2011 Wall shear stress in accelerating turbulent pipe flow. *Journal of Fluid Mechanics* **685**, 440–460.

He, S. & Jackson, J. D. 2000 A study of turbulence under conditions of transient flow in a pipe. *Journal of Fluid Mechanics* **408**, 1–38.

Hutchins, N., Nickels, T. B., Marusic, I. & Chong, M. S. 2009 Hot-wire spatial resolution issues in wall-bounded turbulence. *Journal of Fluid Mechanics* **635**, 103–136.

Jeong, J. & Hussain, F. 1995 On the identification of a vortex. *Journal of Fluid Mechanics* **285**, 69–94.

Jung, S. Y. & Chung, Y. M. 2012 Large-eddy simulations of accelerated turbulent flow in a circular pipe. *International Journal of Heat and Fluid Flow* **33** (1), 1–8.

Maday, Y. & Patera, A. 1989 Spectral element methods for the Navier-Stokes equations. *State of the Art Surveys in Computational Cechanics ASME* pp. 71–143.

Seddighi, M., He, S., Vardy, A. E. & Orlandi, P. 2014 Direct numerical simulation of an accelerating channel flow. *Flow, Turbulence and Combustion* **92** (1-2), 473–502.

Wagner, C., Huttl, T. J. & Friedrich, R. 2001 Low-Reynolds-number effects derived from direct numerical simulations of turbulent pipe flow. *Computers and Fluids* **30** (5), 581–590.

Wu, X. & Moin, P. 2008 A direct numerical simulation study on the mean velocity characteristics in turbulent pipe flow. *Journal of Fluid Mechanics* **608**, 81–112.

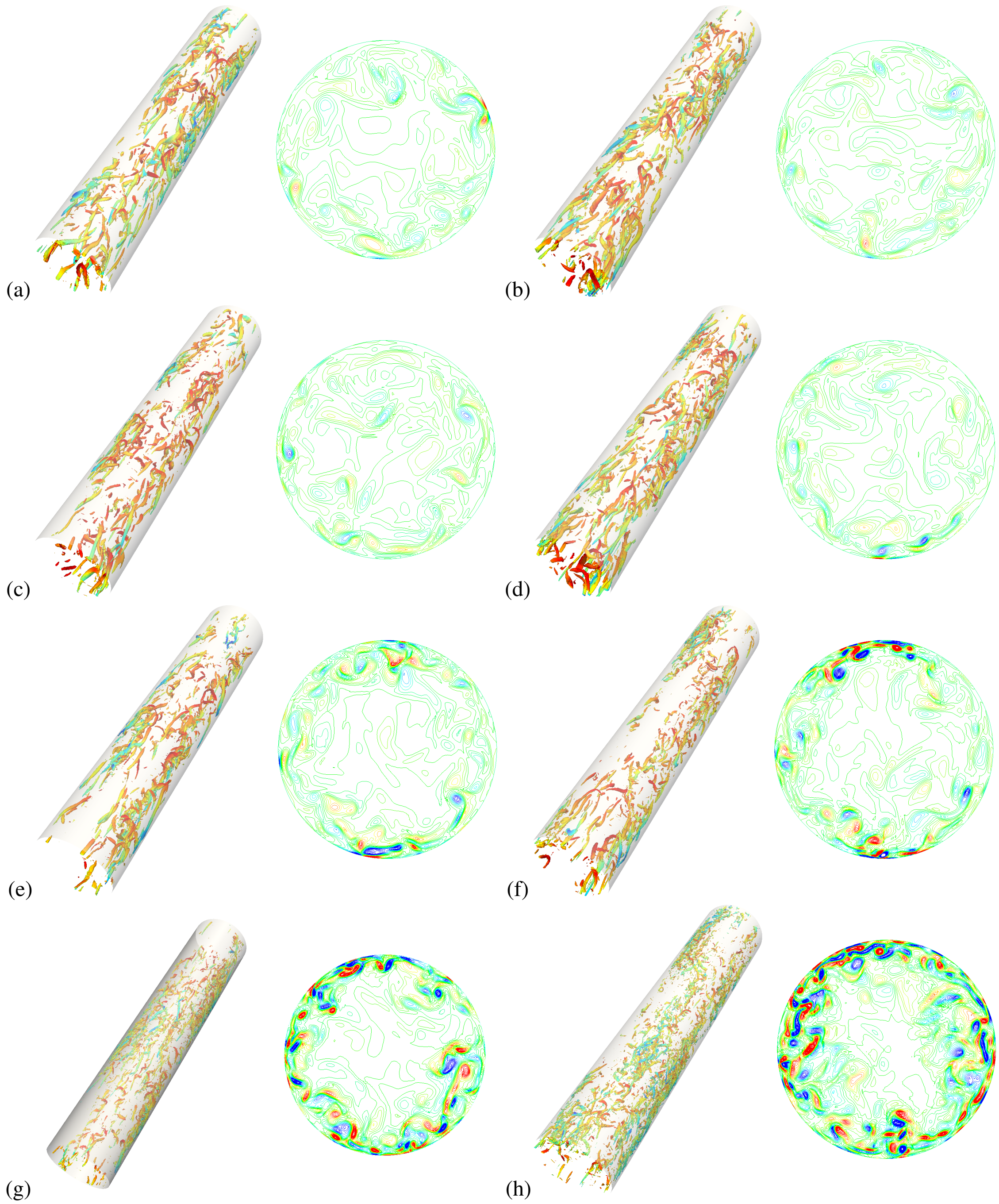

Figure 8. Combined view of λ_2 structures and 2D instantaneous streamwise vorticity in the pipe flow during acceleration. (a) $Re_D = 5300$; (b) $Re_D = 6000$; (c) $Re_D = 7000$; (d) $Re_D = 8000$; (e) $Re_D = 9000$; (f) $Re_D = 10000$; (g) $Re_D = 11000$; (h) $Re_D = 11700$. Local maximum $\lambda'_{2_{rms}}$ value is used for representing the structures and structures are coloured by local instantaneous streamwise velocity. Same contour levels are used for all the 2D instantaneous vorticity plots.